Supplementary Information

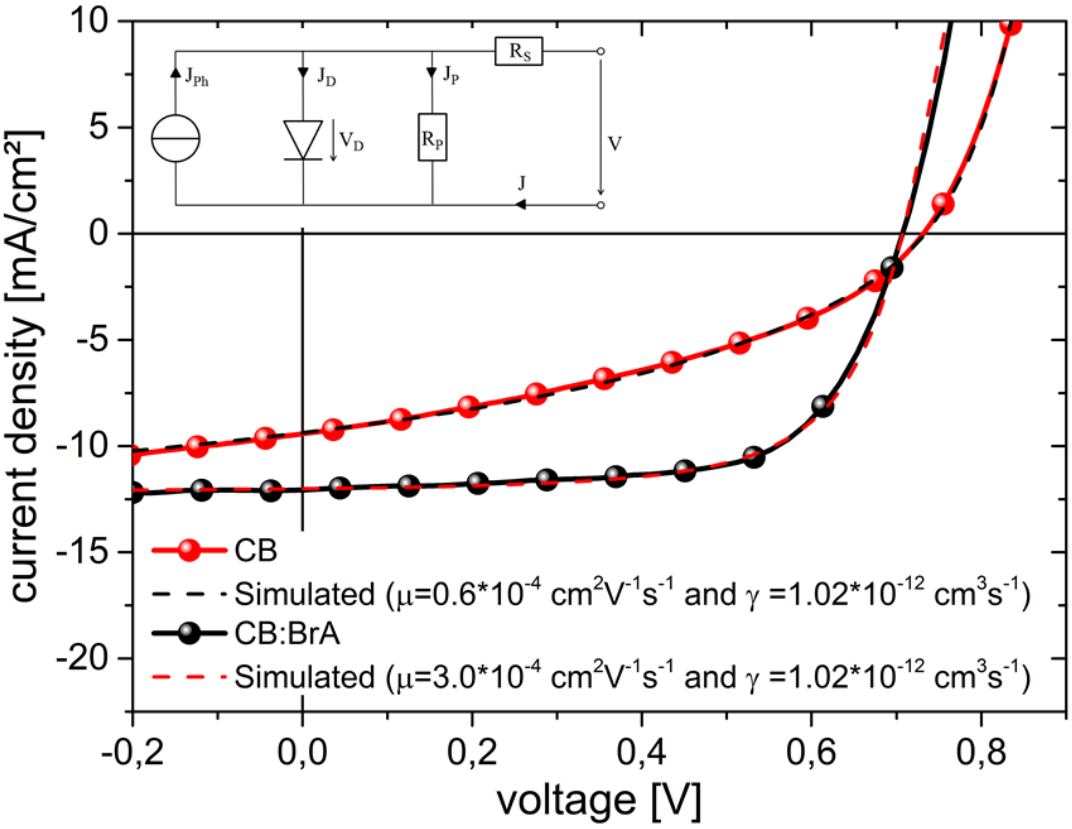

Figure S1
JV-curves of doctor-bladed P3HT:IDTBR solar cells (cell area 0.104 cm²) on glass/ITO substrates processed from neat chlorobenzene (CB) and CB with 5 vol.% p-bromoanisol and fitted simulated curves.

The simulations were performed using the one diode model, which is based on the equivalent circuit shown in **Figure S2**. In this model, the total current J(V) is composed of a current through the diode, a current through the shunt resistor, and the photocurrent J_{ph}:

$$J(V) = J_0\left(exp\left(\frac{q(V-JR_S)}{xkT}\right)-1\right)-\frac{V-JR_S}{R_P}-J_{Ph} \quad (1)$$

Where J_0 is the exchange current, q is the charge, V is the bias voltage applied to the circuit, x is the quality factor of the diode, k is the Boltzmann factor, T is the temperature, R_s and R_p are the serial and the parallel resistances, respectively.

J_{ph} is obtained from the charge carrier balance resulting from generation (G), recombination (R), and extraction, at steady state illumination $\frac{dn}{dt} = G - R - J_{ph}(V) = I_{abs}\cdot\varphi_{ccf} - \gamma\cdot n^2 - \frac{\mu\cdot n\cdot(V-V_{bi})}{d^2} = 0$, assuming that 2nd order recombination dominates, which has been shown to be the case in non-degraded cells.[1] In this equation, I_{abs} represents the intensity of absorbed light, ϕ_{ccf} the efficiency of charge carrier formation, γ the 2nd order recombination coefficient, μ the charge carrier mobility, V_{bi} the built in potential, and d the active layer thickness.

a)

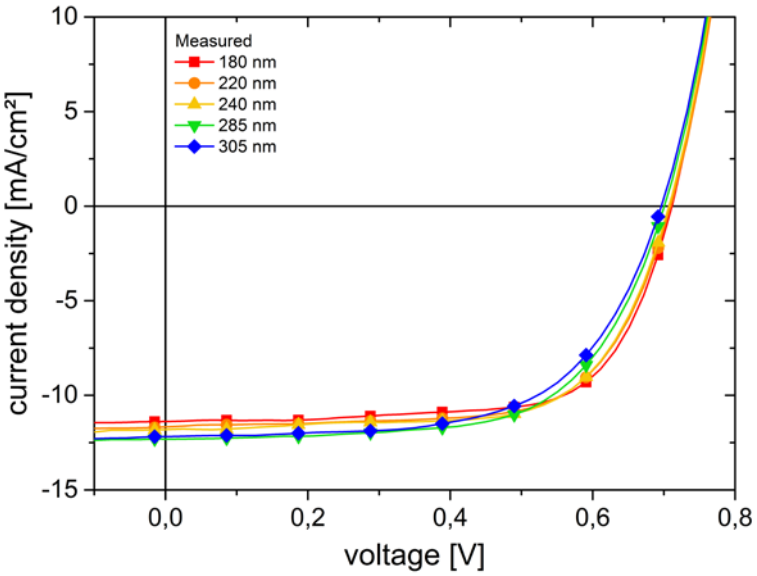

b)

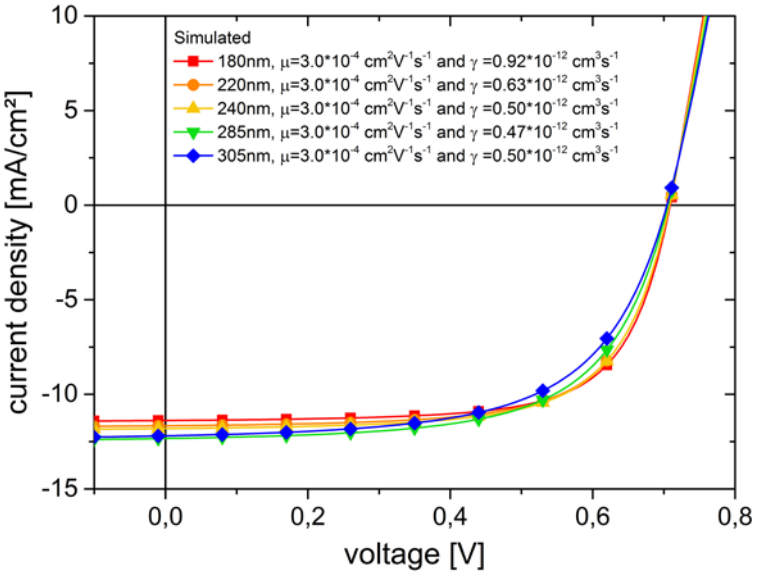

Figure S1

a) JV-curves of doctor-bladed P3HT:IDTBR solar cells (cell area 0.104 cm²) on glass/ITO substrates processed from CB with 5 vol.% p-bromoanisol comprising different active layer thicknesses and b) the simulated counterparts.

In order to find suitable solvents for semiconducting inks, the Hansen solubility parameter approach was used. The solubility parameter δ_T introduced by Hildebrand and Scott is defined as follows:

$$\delta_T = \sqrt{\frac{\Delta H_v - RT}{V}} \tag{2}$$

with ΔH_v as enthalpy of vaporization, R as ideal gas constant, V as molar Volume and T as absolute temperature.[2] A separation of the Hildebrand parameter into the three major corresponding intermolecular contributions leads to the better known Hansen solubility parameters (HSP): the non-polar bonding or dispersion parameter (δd), polar (δp) and hydrogen bonding (δhb) (**Eq. (3)**).[3]

$$\delta_T^2 = \delta_d^2 + \delta_p^2 + \delta_{hb}^2 \tag{3}$$

The material-solvent distance R_a in the Hansen space is described as follows,

$$R_a = \sqrt{4(\delta D_1 - \delta D_2)^2 + (\delta P_1 - \delta P_2)^2 + (\delta H_1 - \delta H_2)^2} \tag{4}$$

where the indexes 1 and 2 denote solute and solvent, respectively.

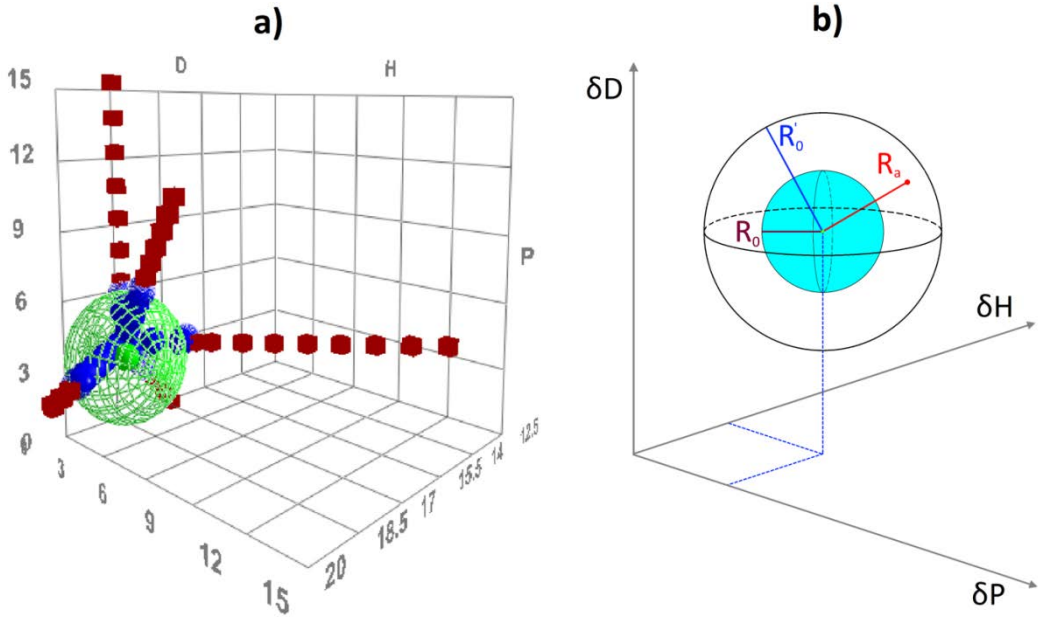

Figure S3

a) Solubility sphere of IDTBR based on binary mixtures of chlorobenzene with 1-butanol, propylene carbonate, cyclohexane, pyrimidine and diiodomethane. The sphere center represents the HSPs of IDTBR and the surface the self-defined solubility limit of 10 mg/mL. Solvents inside the sphere are able to reach solubility >10mg/mL. b) Graphical illustration of temperature dependency of solute solubility, whereby R_0 and R_0' are the radii for T_1 and T_2, respectively ($T_2 > T_1$). A solvent in the distance R_a is able to dissolve the material at T_2, but not at T_1.

In general, the solubility sphere of a material, as shown in **Figure S3**, describes the suitability of a solvent to dissolve the material under consideration, good solvents being located inside and bad solvents being located outside the sphere. The center of the sphere represents the HSPs of the material and the radius R_0 the arbitrarily defined solubility limit (for roll-to-roll application 10 mg/mL). By increasing the temperature, the solubility and thus R_0 increase, which leads to an enhanced number of

suitable solvents (**Figure 3b**). This allows us to find solvents, which are bad solvents at room temperature, but good solvents at the accessible processing temperatures of around 50 - 100 °C.

The Hansen solubility parameters (HSP) of IDTBR were determined via the binary gradient method, which was developed by Machui et al..[4] First, the solubility of IDTBR is tested in binary solvent mixtures consisting of a good solvent (chlorobenzene) and a non-solvent (1-butanol, propylene carbonate, cyclohexane, pyrimidine and diiodomethane) (**Figure S4**). Then an arbitrarily defined solubility limit of 10 mg/mL is used to split the solubility values into "good" (Score=1) and "bad" (Score=0). Finally, the scores are fed into the software HSPiP (v.5.0.03), which uses a quality-of-fit function to generate a solubility sphere (**Figure S3**). The center of the sphere then represents the HSP of the IDTBR with δD = 19.6 $MPa^{0.5}$, δP = 4.6 $MPa^{0.5}$ and δH = 2.9 $MPa^{0.5}$. The HSPs of P3HT at room temperature, δD = 18.5 $MPa^{0.5}$, δP = 4.6 $MPa^{0.5}$ and δH = 1.4 $MPa^{0.5}$, were chosen from reference [4], while the HSPs of the solvents were taken from the database of HSPiP.

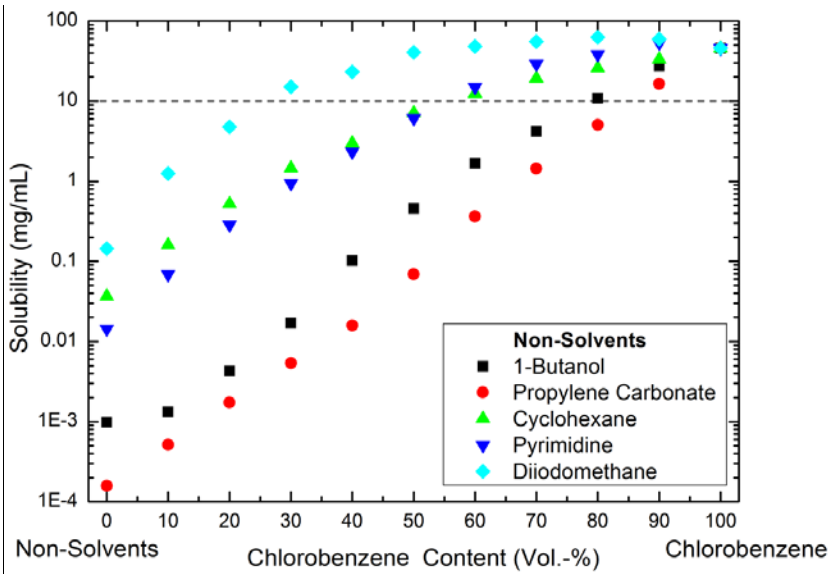

Figure S4

Solubility of IDTBR in binary mixtures of chlorobenzene with 1-butanol, propylene carbonate, cyclohexane, pyrimidine and diiodomethane. The dashed line shows the self-defined solubility limit of 10 mg/mL.

To determine the temperature dependency of the P3HT-Solubility sphere, binary solvent mixtures with R_a values of 2.0 $MPa^{0.5}$, 2.5 $MPa^{0.5}$, 3.0 $MPa^{0.5}$ and 3.5 $MPa^{0.5}$, respectively, were prepared, using the solvents CB:1-butanol, CB:diiodomethane and CB:β-pinene (**Table S1**). Each mixture, containing 10 mg/mL P3HT was heated up until all material was in solution.

At this temperature, R_a is equal to R_0. Together with R_0 = 1.2 $MPa^{0.5}$ at 20 °C, a square root function behavior of R_0 vs. T was found (**Figure S5**), which can be described by the temperature dependency of the Flory-Huggins interaction parameter $\chi_{1,2}$ (Eq. 5-7).

$$\chi_{1,2} = \alpha \frac{v_0}{RT}\left[\left(\delta_{d,1} - \delta_{d,2}\right)^2 + 0.25\left(\delta_{p,1} - \delta_{p,2}\right)^2 + 0.25\left(\delta_{hb,1} - \delta_{hb,2}\right)^2\right] \quad (5)$$

$$\chi_{1,2} = \alpha \frac{v_0}{RT} {R_a}^2 \quad (6)$$

$$R_a = \sqrt{\frac{\chi_{1,2} R}{\alpha v_0}} \cdot \sqrt{T} \quad (7)$$

with α as dimensionless correction constant, R as ideal gas constant, v_0 as molar volume of the solvent and T as absolute temperature. Eq. 5 was implemented by Lindvig et al., proposing an α-value of around 0.6.[5]

Table S1

Solvent combinations (SC) of chlorobenzene (CB) with 1-butanol, diiodomethane (DM) and β-pinene, which represent specific solubility distances (R_a) between P3HT and liquid. For each SC the temperature was identified, at which the SC is able to dissolve 10 mg/mL of P3HT.

R_a [$MPa^{0.5}$]	CB [Vol.-%]	1-Butanol [Vol.-%]	T [°C]	CB [Vol.-%]	DM [Vol.-%]	T [°C]	CB [Vol.-%]	β-Pinene [Vol.-%]	T [°C]	T_Average [°C]
2	90	10	35	88	12	30	60	40	35	33.33
2.5	86	14	50	81	19	45	51	49	50	48.33
3	83	17	65	74	26	60	43	57	65	63.33
3.5	79	21	85	67	33	80	34	66	85	83.33

In order to match the boundary conditions (1) and (2), P3HT-R_0 values of 3.2 $MPa^{0.5}$ (R_0) and 3.6 $MPa^{0.5}$ (R_0') were estimated for 75 °C and 90 °C, respectively, from **Figure S5** Because of HSP inaccuracy, an error of ± 0.2 $MPa^{0.5}$ in R_0 was assumed for further calculations. An in-house database consisting of over 200 environmentally friendlier solvents was used to find solvents, which are in a P3HT-solvent distance range of 3.0-3.8 $MPa^{0.5}$. Assuming that IDTBR (R_0 = 3.7 $MPa^{0.5}$ at 25 °C) has a similar temperature trend, all solvents are expected to show high solubility for IDTBR.

In terms of low-cost production of OPVs, the solvent purchase prices also need to be taken into account. **Figure S6** compares prices for different types of solvents.

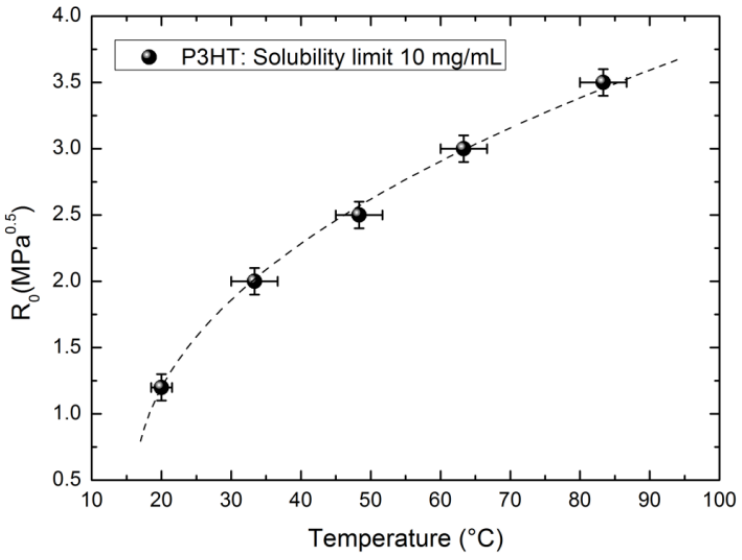

Figure S5

Radius R_0 of the solubility sphere as a function of temperature. The radius is fixed at a solubility limit of 10 mg/mL. The dashed line is a guide to the eye.

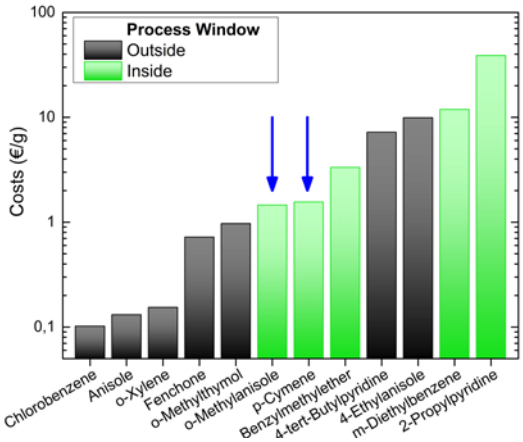

Figure S6

Purchase costs of various solvents. The green colored bars describe solvents which are inside the processing window of **Figure 1**. For device fabrication o-methylanisole and p-cymene were chosen (blue arrow).

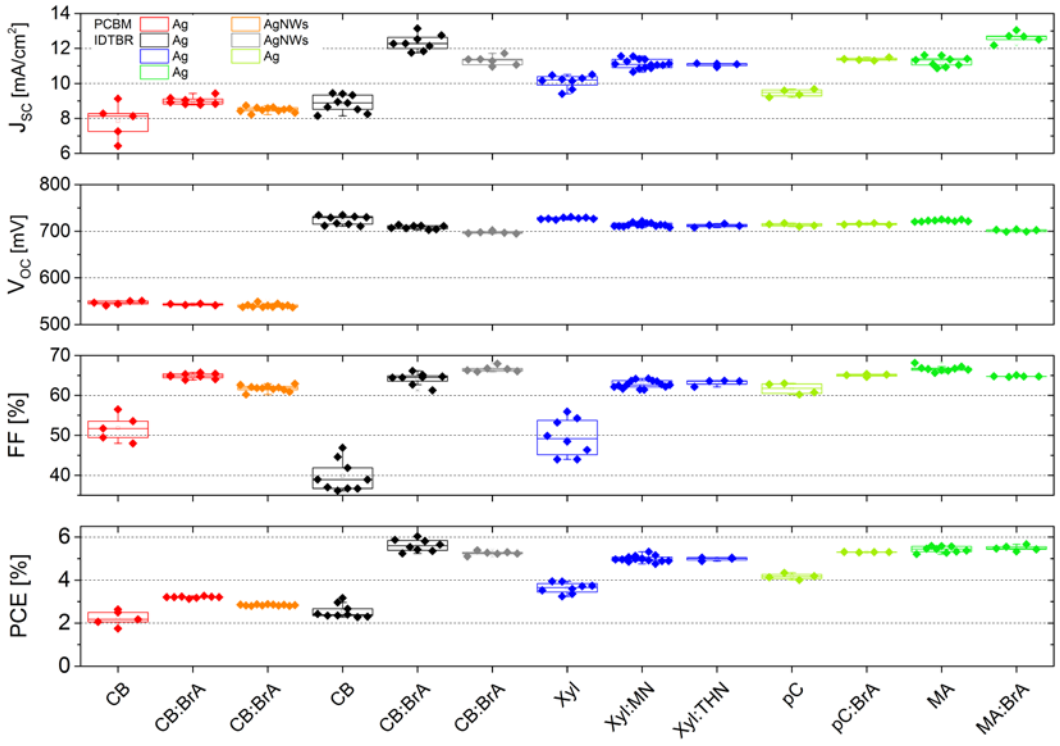

Figure S7

Box plots of the photovoltaic key parameters of doctor-bladed single cell devices with an area of 0.1 cm² on glass/ITO substrates processed with different Acceptor Materials, from different solvent systems and with different top electrodes.

a)

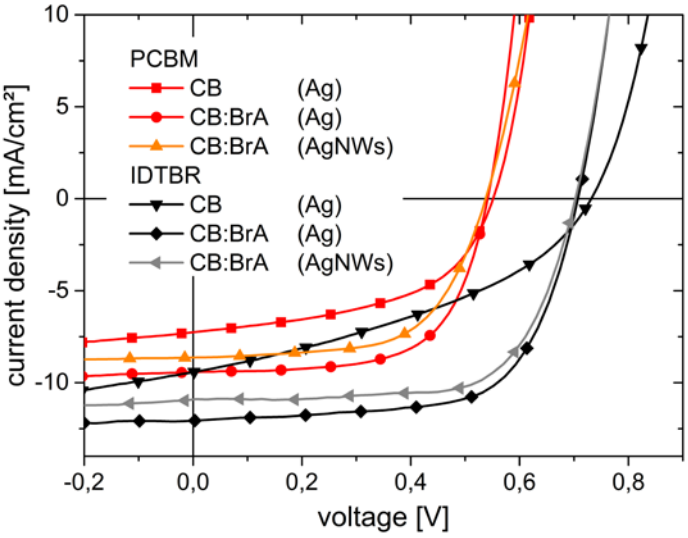

b)

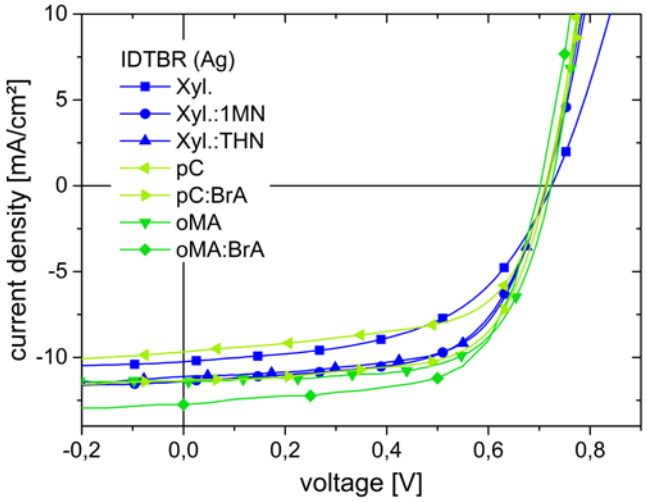

Figure S8

JV-curves of doctor-bladed solar cells (cell area 0.104 cm²) on glass/ITO substrates processed with a) P3HT: PCBM / IDTBR from CB / CB:BrA with Ag and AgNWs top electrode and b) P3HT:IDTBR form different solvents with Ag top electrode.

a)

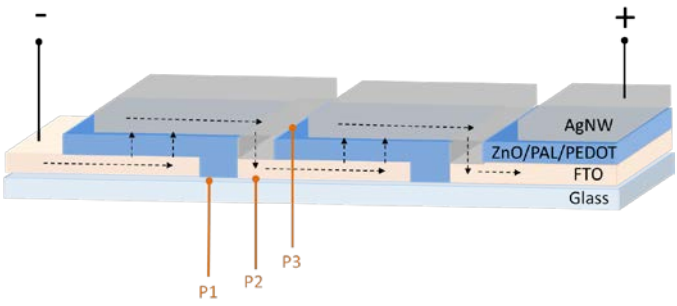

b)

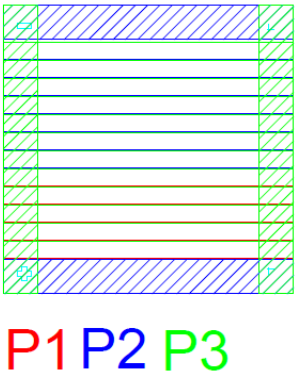

Figure S9

a) Schematic diagram of the module device architecture with the patterning lines P1, P2 and P3. A detailed description of patterning process and the monolithic interconnection can be found in references [6] and [7]. b) Module layout with the structuring lines P1, P2 and P3.

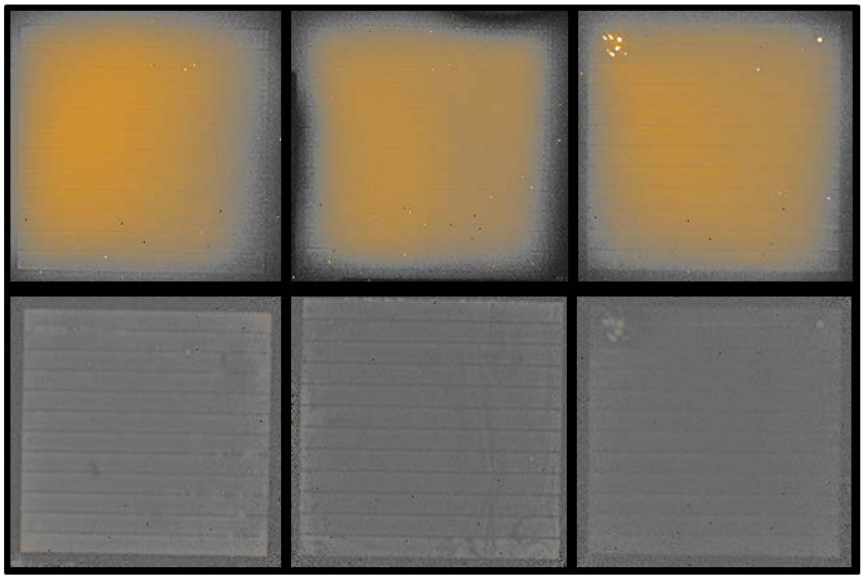

Figure S10

Qualitative Dark Lock-in Thermography (DLIT) amplitude (top) and phase (bottom) images of the best achieved modules of P3HT:IDTBR coated with the doctor blade from CB:BrA solution (first

column), coated with doctor blade from o-MA solution (middle column) and slot-die coated with a slot-die from CB:BrA solution (right column).

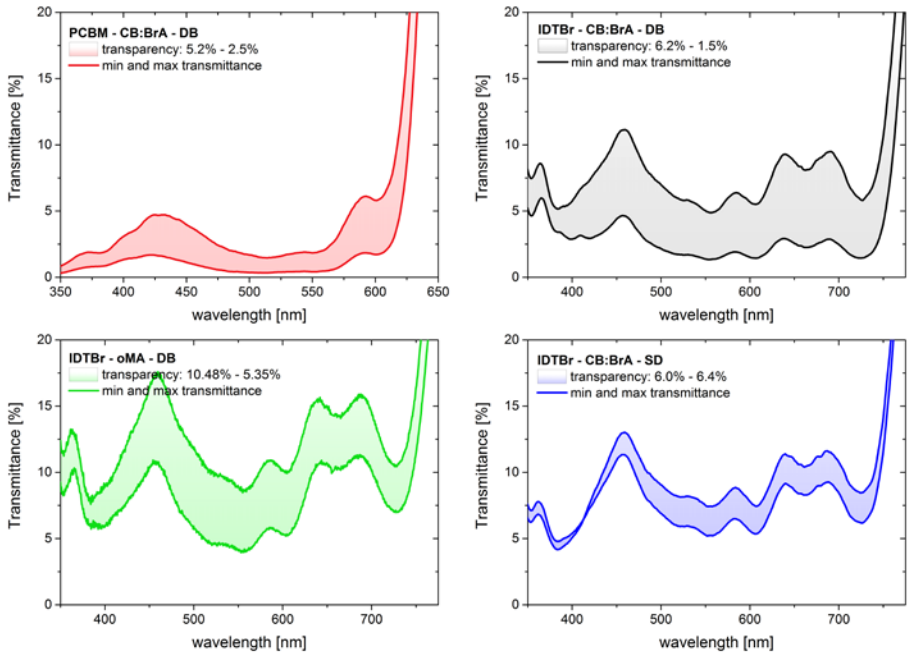

Figure S11

Transmission spectra of doctor bladed (DB) and slot die (SD) coated P3HT: PCBM/IDTBR modules coated on glass/ITO substrates with solution processed AGNWs top electrode. Active layers are processed from CB:BrA or oMA. Transparency values were calculated using the ISO9050-2003.

1 N. Gasparini, M. Salvador, T. Heumueller, M. Richter, A. Classen, S. Shrestha, G. J. Matt, S. Holliday, S. Strohm, H.-J. Egelhaaf, A. Wadsworth, D. Baran, I. Mcculloch and C. J. Brabec, *Adv. Energy Mater.*, 2017, **1701561**, 1–8.

2 J.H. Hildebrand, R.L. Scott, *J. Chem. Phys.*, 1952, **20**, 1520-1521.

3 C. M. Hansen, *Hansen Solubility Parameters A User's Handbook*, 2013, vol. 53.

4 F. Machui, S. Langner, X. Zhu, S. Abbott and C. J. Brabec, *Sol. Energy Mater. Sol. Cells*, 2012, **100**, 138–146.

5 T. Lindvig, M. L Michelsen, G. M Kontogeorgis, *Fluid Phase Equilibria*, 2002, **203**, 247–260.

6 L. Lucera, F. Machui, P. Kubis, H. D. Schmidt, J. Adams, S. Strohm, T. Ahmad, K. Forberich, H.-J. Egelhaaf and C. J. Brabec, *Energy Environ. Sci.*, 2016, **9**, 89–94.

7 P. Kubis, L. Lucera, F. Machui, G. Spyropoulos, J. Cordero, A. Frey, J. Kaschta, M. M. Voigt, G. J. Matt, E. Zeira and C. J. Brabec, *Org. Electron. physics, Mater. Appl.*, 2014, **15**, 2256–2263.